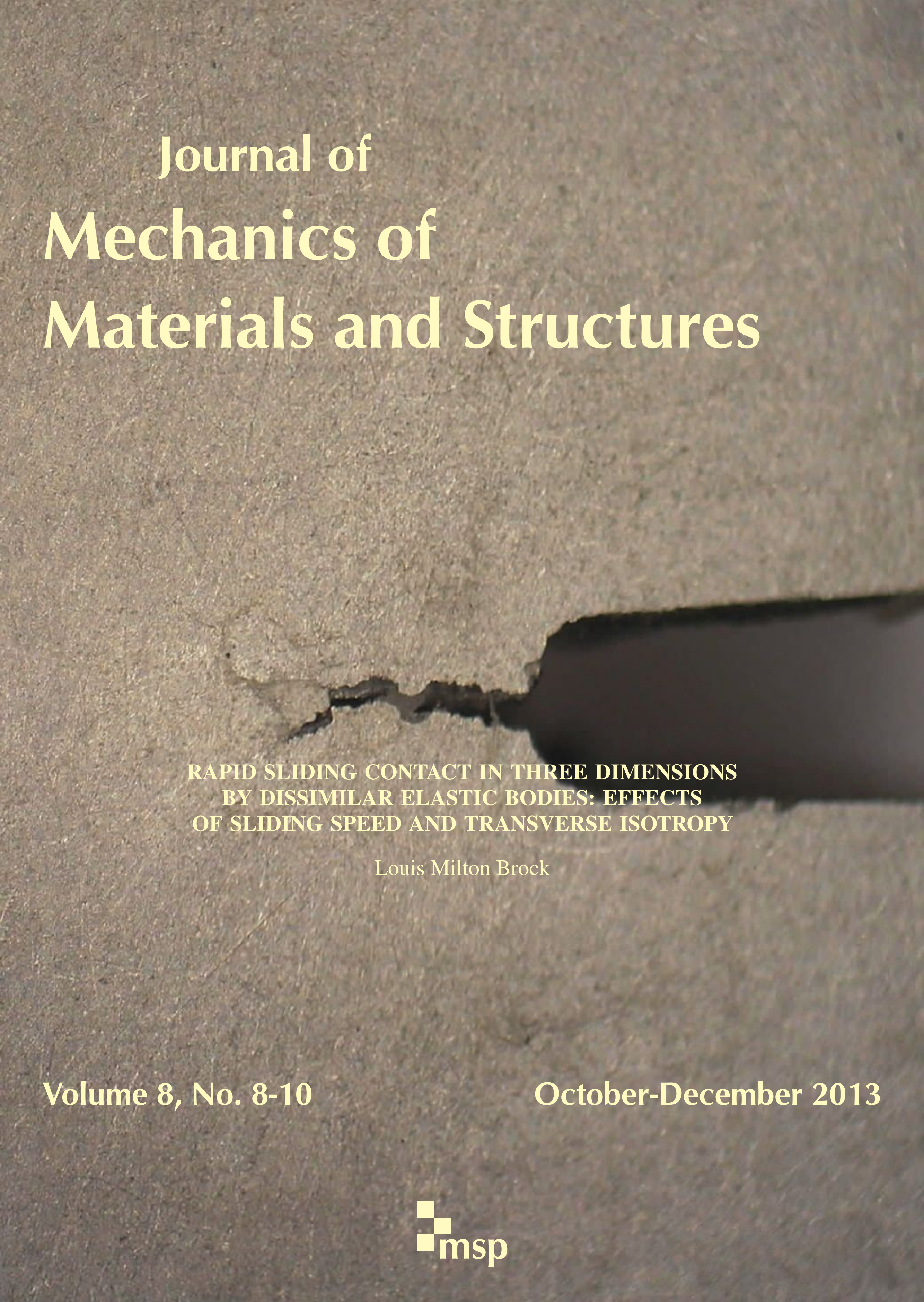

Journal of
Mechanics of
Materials and Structures

RAPID SLIDING CONTACT IN THREE DIMENSIONS BY DISSIMILAR ELASTIC BODIES: EFFECTS OF SLIDING SPEED AND TRANSVERSE ISOTROPY

Louis Milton Brock

Volume 8, No. 8-10 October-December 2013

msp

JOURNAL OF MECHANICS OF MATERIALS AND STRUCTURES
Vol. 8, No. 8-10, 2013
dx.doi.org/10.2140/jomms.2013.8.461

msp

RAPID SLIDING CONTACT IN THREE DIMENSIONS BY DISSIMILAR ELASTIC BODIES: EFFECTS OF SLIDING SPEED AND TRANSVERSE ISOTROPY

LOUIS MILTON BROCK

An isotropic elastic sphere slides on the surfaces of transversely isotropic elastic half-spaces. In one case the material symmetry axis coincides with the half-space surface normal. In the other, the axis lies in the plane of the surface. In both cases sliding proceeds with constant subcritical speed along a straight path at an arbitrary angle to the principal material axes. A 3D dynamic steady state is considered. Exact solutions for contact zone traction are derived in analytic form, as well as formulas for contact zone geometry. Although a sphere is involved, the solution process is not based on the assumption of symmetry. Anisotropy is found to largely determine zone shape at low sliding speed, but direction of sliding becomes a major influence at higher speeds.

1. Introduction

The literature on the mechanics of contact is vast; see, for example, [Johnson 1985; Kalker 1990; Hills et al. 1993]. An important category is contact between dissimilar elastic bodies; see, for example, [Hertz 1882; Hartnett 1980; Ahmadi et al. 1983; Hills et al. 1993]. For sliding contact, if speed and resultant forces are constant, a dynamic steady state may be achieved for which contact zone and surface traction do not vary in the frame of the moving sphere. In [Brock 2012] the 3D problem of rapid sliding by a rigid ellipsoidal die on an isotropic half-space in the presence of friction is studied. Analytical solutions show that contact zone shape does not necessarily replicate a projection of the die profile onto the half-space surface. As sliding speed increases, the shape elongates in the direction of sliding, a result also seen in [Rahman 1996]. This problem is generalized by considering a transversely isotropic half-space [Brock 2013] and a die that slides in any direction with respect to the principal axes of the material. Again, contact zone shape may not replicate the die profile projection, but for low sliding speeds it is largely defined in terms of the principal axes. For higher speeds, the elongation effect seen in [Brock 2012] is exhibited. That is, as speed increases, the zone appears to rotate while undergoing elongation. In contrast to [Brock 2012], moreover, the Rayleigh speed may not be critical.

To ascertain whether the results of [Brock 2012; 2013] are a phenomenon of the rigid die, aspects of both studies are adapted here for two 3D cases of sliding by an isotropic elastic sphere on a transversely isotropic half-space. It is assumed (compare [Hills et al. 1993]) that the maximum contact zone width is much smaller than the radius r_0 of the sphere prior to deformation. Thus, the sphere is also treated as a half-space. With regard to the transversely isotropic half-space, the material symmetry axis is normal to the surface in one case, but lies in the plane of the surface in the other [Brock 2013]. In both cases, the sphere slides in an arbitrary direction with respect to the principal material axes. Sliding can be resisted

Keywords: 3D dynamic, sliding, transverse isotropy, contact zone geometry.

by friction, and sliding speeds are constant and subcritical. The solution for the unmixed boundary value problem of specified surface traction reduces the mixed contact problem to the solution of integral equations. To this end, governing equations for the elastic half-space, subjected to a translating zone of (somewhat) arbitrary traction over its surface, are given in Appendix A and in Section 2. Translation speed is constant and subcritical, and zone geometry and traction do not change during translation. Therefore, see [Brock 2012; 2013], a dynamic steady state is assumed. Cartesian coordinates are used, and an exact transform solution is obtained. Quasipolar coordinates, both in transform and spatial planes, are employed during the inversion process. These are defined by a polar angle that sweeps through 180° (π radians) and a radial coordinate that has both positive and negative directions. For points in the contact zone, the resulting displacement expressions reduce to double integrals whose limits are independent of the points. The imposed displacement conditions require that the integrands be solutions of Cauchy singular integral equations. The contact zone normal traction is then extracted analytically as a function of the quasipolar coordinates. This traction is required to vanish continuously on the contact zone boundary, and to render the resultant compression force as a stationary value for a given sliding speed. These requirements lead to expressions that define the contact zone geometry, and calculations for aspects of the geometry are given.

Solution expressions for anisotropic elasticity are often [Ting 1996] more complicated than for their isotropic counterparts. A cancellation of common factors in the numerator and denominator of solution transform terms is used for the 2D [Brock 2002] and 3D [Brock 2013] problems. The resulting expressions yield, upon inversion, more compact solution forms. The procedure is therefore used here for both the isotropic and transversely isotropic components of the transform solution.

2. General equations for the traction distribution problem

A linear elastic, anisotropic, and homogeneous half-space is defined as the region $x_3 > 0$. Here Cartesian coordinates $\boldsymbol{x}(x_k)$ also define the principal axes of the material. The half-space is undisturbed until a traction distribution is applied to a finite, simply connected area C of surface $x_3 = 0$. Its boundary is defined by contour $\Im(X, Y) = 0$, where

$$X = x_1 \cos\theta + x_2 \sin\theta, \quad Y = x_2 \cos\theta - x_1 \sin\theta, \quad |\theta| < \pi/2. \tag{1}$$

Here $\Im = 0$ defines a continuous closed curve that exhibits continuously varying tangent direction, and normal direction, and radius of curvature. Moreover, any span of C through origin $x_1 = x_2 = 0$ does not cross its boundary. Area C is then translated in the positive X-direction at constant subcritical speed V. This does not change the area, and the traction distribution remains invariant with respect to it. This suggests that a dynamic steady state can arise in which half-space response is invariant in the frame of translating C. It is therefore convenient to translate the Cartesian system with C, so that displacement $\boldsymbol{u}(u_k)$ and traction $\boldsymbol{T}(\sigma_{ik})$ vary with $\boldsymbol{x}(x_k)$ and time differentiation becomes $-V\partial_X$, where ∂_X signifies the X-derivative and is given by

$$\partial_X = \partial_1 \cos\theta + \partial_2 \sin\theta. \tag{2}$$

Here ∂_k signifies x_k-differentiation. The governing equations for the general anisotropic solid are given in Appendix A. For $x_3 = 0$ the boundary conditions are

$$\sigma_{33} = \sigma, \quad \sigma_{31} = \tau_1, \quad \sigma_{32} = \tau_2, \quad (x_1, x_2) \in C, \tag{3a}$$

$$\sigma_{33} = \sigma_{31} = \sigma_{32} = 0, \qquad (x_1, x_2) \notin C. \tag{3b}$$

Here (σ, τ_1, τ_2) are piecewise continuous, bounded functions of (x_1, x_2). It is reasonable then to require that $|\boldsymbol{u}|$ remains bounded for $x_3 > 0$, $|\boldsymbol{x}| \to \infty$.

3. Transverse isotropy: Material symmetry axis normal to surface

Traction distribution problem: Transform. For this case the results in Appendix A involve five elastic constants [Jones 1999]:

$$C_{22} = C_{11}, \quad C_{44} = C_{55}, \quad C_{23} = C_{13}, \quad C_{33}, \quad C_{11} - C_{12} - 2C_{66} = 0. \tag{4}$$

The spherical die is isotropic, with only two elastic constants, so it is convenient to use its shear modulus μ_0, mass density ρ_0, and rotational wave speed v_0 as reference parameters, where

$$v_0 = \sqrt{\frac{\mu_0}{\rho_0}}. \tag{5}$$

Dimensionless parameters can then be defined:

$$d_1 = \frac{C_{11}}{\mu_0}, \quad d_3 = \frac{C_{33}}{\mu_0}, \quad d_5 = \frac{C_{55}}{\mu_0}, \quad d_6 = \frac{C_{66}}{\mu_0}, \quad d_{12} = \frac{C_{12}}{\mu_0}, \quad d_{13} = \frac{C_{13}}{\mu_0}, \tag{6a}$$

$$d_1 - d_{12} - 2d_6 = 0, \quad c = \sqrt{\frac{\rho}{\rho_0}}c_0, \quad c_0 = \frac{V}{v_0}. \tag{6b}$$

In view of (A.3) and (6) the linear momentum balance (A.5a) takes the form

$$\begin{bmatrix} d_5\partial_3^2 + \mathrm{X}_1 & (d_6+d_{12})\partial_1\partial_2 & (d_5+d_{13})\partial_1\partial_3 \\ (d_6+d_{12})\partial_1\partial_2 & d_5\partial_3^2 + \mathrm{X}_2 & (d_5+d_{13})\partial_2\partial_3 \\ (d_5+d_{13})\partial_1\partial_3 & (d_5+d_{13})\partial_2\partial_3 & d_3\partial_3^2 + \mathrm{X}_3 \end{bmatrix} \begin{bmatrix} u_1 \\ u_2 \\ u_3 \end{bmatrix} = 0, \tag{7a}$$

$$\mathrm{X}_1 = d_1\partial_1^2 + d_6\partial_2^2 - c^2\partial_X^2, \quad \mathrm{X}_2 = d_6\partial_1^2 + d_1\partial_2^2 - c^2\partial_X^2, \quad \mathrm{X}_3 = d_5(\partial_1^2 + \partial_2^2) - c^2\partial_X^2. \tag{7b}$$

The set of (3) and (7) is addressed by the double bilateral Laplace transform [Sneddon 1972]:

$$\hat{F} = \iint F(x_1, x_2)\exp(-p_1x_1 - p_2x_2)\,dx_1\,dx_2. \tag{8}$$

In (8) integration is over the entire x_1x_2-plane and transform variables (p_1, p_2) are imaginary. Its application to (7) for $x_3 > 0$ leads to the homogeneous solution

$$\hat{\boldsymbol{u}} = \boldsymbol{U}_+\exp(-\Omega_+x_3) + \boldsymbol{U}_-\exp(-\Omega_-x_3) + \boldsymbol{U}_6\exp(-\Omega_6x_3). \tag{9}$$

Exponential arguments $(\Omega_\pm, \Omega_6)$ are roots of the determinant of transformed (7a), that is,

$$(\Omega^2+\omega_6^2)[(d_5\Omega^2+\omega_1^2)(d_3\Omega^2+\omega_5^2)-\Omega^2 P(d_5+d_{13})^2]=0, \tag{10a}$$

$$\omega_1=\sqrt{d_1P-c^2p_X^2},\quad \omega_5=\sqrt{d_5P-c^2p_X^2},\quad \omega_6=\sqrt{d_6P-c^2p_X^2}, \tag{10b}$$

$$P=p_1^2+p_2^2,\quad p_X=p_1\cos\theta+p_2\sin\theta. \tag{10c}$$

They are given by

$$\Omega_\pm=\frac{\omega_+\pm\omega_-}{2\sqrt{d_3d_5}}\sqrt{-1},\quad \Omega_6=\omega_6\sqrt{-1}, \tag{11a}$$

$$\omega_\pm=\sqrt{\left(\omega_1\sqrt{d_3}\pm\omega_5\sqrt{d_5}\right)^2-P(d_5+d_{13})^2}, \tag{11b}$$

$$\Omega_+\Omega_-=-\frac{\omega_1\omega_5}{\sqrt{d_3d_5}}. \tag{11c}$$

The components of the vector coefficients $(\boldsymbol{U}_\pm, \boldsymbol{U}_6)$ in (9) are

$$(U_1^\pm, U_2^\pm)=(d_5+d_{13})(p_1,p_2)\Omega_\pm U_\pm,\quad U_3^\pm=(d_5\Omega_\pm^2+\omega_1^2)U_\pm, \tag{12a}$$

$$U_1^6=-p_2U_6,\quad U_2^6=p_1U_6,\quad U_3^6=0. \tag{12b}$$

Here $(U_\pm, U_6)$ are arbitrary functions of (p_1, p_2). Result (9) is bounded for $x_3>0$ if $\mathrm{Re}(\Omega_++\Omega_-, \Omega_+-\Omega_-, \omega_1, \omega_5, \omega_6)>0$ in the cut p_1 and p_2-planes. Use of (A.1), (6), (9), and (12) gives the traction transforms for $x_3=0$:

$$\frac{1}{\mu_0}\begin{bmatrix}\hat\sigma_{33}\\ \hat\sigma_{31}\\ \hat\sigma_{32}\end{bmatrix}=\begin{bmatrix}C_3^+\Omega_+ & C_3^-\Omega_- & 0\\ d_5p_1D_3^+ & d_5p_1D_3^- & d_5p_2\Omega_6\\ d_5p_2D_3^+ & d_5p_2D_3^- & -d_5p_1\Omega_6\end{bmatrix}\begin{bmatrix}U_+\\ U_-\\ U_6\end{bmatrix}, \tag{13a}$$

$$C_3^\pm=d_{13}(d_5+d_{13})P-d_3(d_5\Omega_\pm^2+\omega_1^2),\quad D_3^\pm=\omega_1^2-d_{13}\Omega_\pm^2. \tag{13b}$$

Use of (13) in the transform of (3) gives equations for $(U_\pm, U_6)$. Application of the traction distribution solution to the sliding contact problem requires the normal displacement u_3^0 on surface $x_3=0$. Equation (9) and the solutions for $(U_\pm, U_6)$ are combined in Appendix B to construct its transform $\hat u_3^0$. The construction involves a factor cancellation procedure similar to that used in [Brock 2002; 2013] and some isotropic limit results are also given. In light of (11), (B.2b), and (B.3b), then, one can write the compact expressions for, respectively, the transversely isotropic and isotropic half-spaces:

$$\hat u_3^0=-\frac{\omega_1\omega_+\sqrt{-1}}{\sqrt{d_3d_5}M}\frac{\hat\sigma}{\mu_0}+\frac{N}{M}\left(p_1\frac{\hat\tau_1}{\mu_0}+p_2\frac{\hat\tau_2}{\mu_0}\right), \tag{14a}$$

$$(\hat u_3^0)'=-\frac{c_D^2\omega_D}{M_0\sqrt{-1}}(\omega_D+\omega)\frac{\hat\sigma'}{\mu_0}+\frac{N_0}{M_0}\left(p_1\frac{\hat\tau_1'}{\mu_0}+p_2\frac{\hat\tau_2'}{\mu_0}\right), \tag{14b}$$

$$M_0=4(c_D^2-1)\omega-c_D^2(\omega_D+\omega)c_0^2p_X^2,\quad N_0=c_D^2\omega_D+(2-c_D^2)\omega. \tag{14c}$$

Traction distribution problem: Transform inversion. In view of (7) and [Sneddon 1972] the inversion operation for each traction term in (14) has the general form

$$\frac{1}{2\pi i}\int dp_1 \frac{1}{2\pi i}\int dp_2 C_\Sigma \iint_C d\xi_1\, d\xi_2\, \Sigma \exp[p_1(x_1-\xi_1)+p_2(x_2-\xi_2)]. \tag{15}$$

In (15), $\Sigma = \Sigma(\xi_1, \xi_2)$ is a given traction term in (14) and $C_\Sigma = C_\Sigma(p_1, p_2)$ is its coefficient, for example, $C_\Sigma = Np_1/\mu_0 M$ for $\Sigma = \hat{\tau}_1$ in (14a). Integration is along the entire $\mathrm{Im}(p_1)$ and $\mathrm{Im}(p_2)$-axes, and suggests the transformations [Brock 2012; 2013]

$$p_1 = p\cos\psi, \qquad p_2 = p\sin\psi, \tag{16a}$$

$$x = x_1\cos\psi + x_2\sin\psi, \qquad y = x_2\cos\psi - x_1\sin\psi, \tag{16b}$$

$$\xi = \xi_1\cos\psi + \xi_2\sin\psi, \qquad \eta = \xi_2\cos\psi - \xi_1\sin\psi. \tag{16c}$$

In (16), $\mathrm{Re}(p) = 0+$, $-\infty < [\mathrm{Im}(p), x, y, \xi, \eta, \xi_1, \xi_2] < \infty$, and $|\psi-\theta| < \pi/2$. Parameters (p, ψ), $(x, \psi;\, y = 0)$, and $(\xi, \psi;\, \eta = 0)$ constitute quasipolar coordinate systems, that is,

$$dx_1\, dx_2 = |x|\, dx\, d\psi, \quad d\xi_1\, d\xi_2 = |\xi|\, d\xi\, d\psi, \quad dp_1\, dp_2 = |p|\, dp\, d\psi. \tag{17}$$

Use of (16a) in (11) and (12) leads to formulas related to (14a):

$$\Omega_\pm = B_\pm\sqrt{-p^2}, \quad \Omega_6 = B_6\sqrt{-p^2}, \tag{18a}$$

$$\omega_1 = A_1 p, \quad \omega_5 = B_5 p, \quad \omega_6 = B_6 p, \tag{18b}$$

$$\omega_\pm = \mathrm{P}_\pm p, \quad M = \mathrm{M}p^3, \quad N = \mathrm{N}p^2, \quad P = p^2. \tag{18c}$$

Equation (18) involves dimensionless terms

$$B_\pm = \frac{\mathrm{P}_+ \pm \mathrm{P}_-}{2\sqrt{d_3 d_5}}, \quad \mathrm{P}_\pm = \sqrt{\left(\sqrt{d_3}A_1 \pm \sqrt{d_5}B_5\right)^2 - (d_5+d_{13})^2}, \tag{19a}$$

$$A_1 = \sqrt{d_1 - c_X^2}, \quad B_5 = \sqrt{d_5 - c_X^2}, \quad B_6 = \sqrt{d_6 - c_X^2}, \quad c_X = c\cos(\psi-\theta), \tag{19b}$$

$$\mathrm{M} = A_1 B_5\left(B_5 + \sqrt{\frac{d_3}{d_5}}A_1\right) - d_5 A_1 - \frac{d_{13}^2 B_5}{\sqrt{d_3 d_5}}, \quad \mathrm{N} = A_1 - \frac{d_{13}B_5}{\sqrt{d_3 d_5}}. \tag{19c}$$

For (14b)

$$\omega_D = Ap, \quad \omega = Bp, \quad M_0 = \mathrm{M}_0 p^3, \quad N_0 = \mathrm{N}_0 p^2, \tag{20a}$$

$$A = \sqrt{1 - \left(\frac{c_X^0}{c_D}\right)^2}, \quad B = \sqrt{1-(c_X^0)^2}, \quad c_X^0 = c_0\cos(\psi-\theta), \tag{20b}$$

$$\mathrm{M}_0 = 4(c_D^2-1)B - c_D^2(A+B)(c_X^0)^2, \quad \mathrm{N}_0 = c_D^2 A + (2-c_D^2)B. \tag{20c}$$

Critical speed. The terms in (19) are functions of $\psi-\theta$. Because $c_X < c$, both B_+ and A_1 are real and positive for $0 < c < \sqrt{d_1}$, and vanish at branch point $c_X = \sqrt{d_1}$. Terms (N, B_-, B_5) are real and positive for $0 < c < \sqrt{d_5}$ and (B_-, B_5) vanish at branch point $c_X = \sqrt{d_5}$. In addition, $\mathrm{M} \to 0+$ when $c_X = 0$ and vanishes for $c_X = (c_X)_R$, $0 < (c_X)_R < \sqrt{d_5}$, that is, M and $(c_X)_R$ correspond to a Rayleigh function and its nonzero root; see Appendix B. For $\psi = \theta$ this root gives the dimensionless Rayleigh speed c_R.

Although not present in (14a), term Ω_6 does appear in $(\hat{u}_1^0, \hat{u}_2^0)$, and its counterpart B_6 vanishes at branch point $c_X = \sqrt{d_6}$. Parameter $c_X^0 < c_0$ and (A, B) in (20) are real for, respectively, $c_0 < c_D$ and $c_0 < 1$. Term M_0 exhibits root $c_X^0 = (c_X^0)_R$ (see Appendix B) that gives Rayleigh speed $(c_0)_R$ when $\psi = \theta$. In summary, if sliding speed V is such that c or c_0 exceed a branch-point value, the corresponding term becomes imaginary, which represents a transonic situation, as in [Brock 2002; 2012; 2013]. If c or c_0 reaches its Rayleigh value, then (14a) or (14b) is singular. Thus, the critical sliding speed is here defined as the maximum V such that (c, c_0) do not exceed any branch point or Rayleigh values. It is noted that the possibility of a non-Rayleigh critical speed does not arise in the plane strain analysis of transverse isotropy, as in [Brock 2002].

Inversion for subcritical speed. In light of (16)–(20), general result (15) takes the form

$$\iint_C \Sigma\, d\xi\, d\eta \frac{1}{\pi i} \int_\Psi C_\Sigma\, d\psi \frac{1}{2\pi i} \int \frac{|p|}{p}\left(1, \frac{\sqrt{-p}}{\sqrt{p}}\right) \exp p(x-\xi)\, dp. \tag{21}$$

Now $\Sigma = \Sigma(\xi, \eta)$, $C_\Sigma = C_\Sigma(\psi, c_X)$, or $C_\Sigma = C_\Sigma(\psi, c_X^0)$, and subscript Ψ signifies integration over the range $\theta - \pi/2 < \psi < \theta + \pi/2$. The p-integration is over the positive side of the entire $\mathrm{Im}(p)$-axis (see Appendix B). For $(x_1, x_2) \in C$ the inverses of (14) follow as

$$u_3^0 = -\frac{1}{\pi} \int_\Psi d\psi \int_{\mathrm{N}} d\eta \left[\frac{A_1 \mathrm{P}_+}{\mu_0 \mathrm{M}\sqrt{d_3 d_5}\pi}(vp) \int_\Xi \sigma(\xi, \eta) \frac{d\xi}{\xi - x} + \frac{\mathrm{N}}{\mu_0 \mathrm{M}} \mathrm{T}(x, \eta)\right], \tag{22a}$$

$$(u_3^0)' = -\frac{1}{\pi} \int_\Psi d\psi \int_{\mathrm{N}} d\eta \left[\frac{c_D^2 A(A+B)}{\mu_0 \mathrm{M}_0 \pi}(vp) \int_\Xi \sigma'(\xi, \eta) \frac{d\xi}{\xi - x} + \frac{\mathrm{N}_0}{\mu_0 \mathrm{M}_0} \mathrm{T}'(x, \eta)\right], \tag{22b}$$

$$\mathrm{T}(\xi, \eta) = \tau_1(\xi, \eta) \cos\psi + \tau_2(\xi, \eta) \sin\psi, \tag{22c}$$

$$\mathrm{T}'(\xi, \eta) = \tau_1'(\xi, \eta) \cos\psi + \tau_2'(\xi, \eta) \sin\psi. \tag{22d}$$

Here (vp) signifies principal value integration and (N, Ξ) signify integration over the ranges $\eta_-(\psi) < \eta < \eta_+(\psi)$ and $x_-(\eta, \psi) < \xi < x_+(\eta, \psi)$, respectively. Limits $\eta_\pm(\psi)$ are points on the contour $\Im[X(\xi, \eta), Y(\xi, \eta)] = 0$ where $d\eta/d\xi = 0$, and limits $x_\pm(\eta, \psi)$ locate the ends of a line parallel to the ξ-axis that spans C for a given η. The restrictions on $(C, \Im)$ imply that $(x_\pm, \eta_\pm)$ exist and are continuous in ψ.

Sliding contact with friction. It is assumed that the maximum deflections of the half-space and sphere surfaces caused by mutual indentation during sliding, and the maximum width of the resulting contact zone, are orders of magnitude less than the original radius r_0 of the sphere. Thus (22b) is a valid approximation for a sphere. For both (22a) and (22b), the contact zone translates in the positive X-direction and $x_3 < 0$ defines the outward normal to the surface. Thus, the condition on $x_3 = 0$ that the deformed surfaces of the two bodies conform in the contact zone can be written for small deformations as

$$u_3^0 + (u_3^0)' = U_3 - \frac{X^2}{2r_0}(x_1, x_2) \in C. \tag{23}$$

The form of (23) is based on measuring (x_1, x_2) from the center of the translating sphere in its rest configuration. Thus U_3 is the rigid-body normal displacement of the sphere, and $(x_1, x_2) = 0$ is the initial contact point. If sliding is resisted by friction with kinetic coefficient γ, and sphere sliding and slip are assumed to coincide, the resultant force system on the sphere is (F_X, F_Y, F_3) where $F_X = \gamma F_3$ and $F_Y = 0$. Thus in (22)

$$\tau_1 = \tau_X \cos\theta, \qquad \tau_2 = \tau_X \sin\theta, \qquad \tau_X = \gamma\sigma \quad (\sigma < 0), \tag{24a}$$

$$\tau_1' = -\tau_X \cos\theta, \quad \tau_2' = -\tau_X \sin\theta, \quad \sigma' = \sigma. \tag{24b}$$

In view of (1), (16), and (24), (23) becomes

$$-\frac{1}{\mu\pi}\int_\Psi d\psi \int_{\mathrm{N}} d\eta \left[\frac{\mathrm{K}}{\pi}(vp)\int_\Xi \sigma(\xi,\eta)\frac{d\xi}{\xi - x} + \Gamma\sigma(x,\eta)\right] = U_3 - \frac{X^2}{2r_0}, \tag{25a}$$

$$\mathrm{K} = \frac{A_1 \mathrm{P}_+}{\mathrm{M}\sqrt{d_3 d_5}} + \frac{c_D^2 A}{\mathrm{M}_0}(A+B), \tag{25b}$$

$$\Gamma = \gamma\left(\frac{\mathrm{N}}{\mathrm{M}} + \frac{\mathrm{N}_0}{\mathrm{M}_0}\right)\cos(\psi - \theta). \tag{25c}$$

In light of (16) and Appendix B the right-hand side of (25a) can be written as

$$-\frac{1}{\pi}\int_\Psi d\psi \int_{\mathrm{N}} d\eta \int_\Xi d\xi \frac{d}{dx}\delta(x-\xi)\left[U_3 - \frac{1}{2r_0}X^2(\xi,\eta)\right], \tag{26a}$$

$$X(\xi,\eta) = \xi\cos(\psi-\theta) + \eta\sin(\psi-\theta). \tag{26b}$$

Here δ is the Dirac function, and so (25a) reduces to matching the integrands of double integration in (ψ, η). Parameter ξ in $\sigma(\xi, \eta)$ is an integration variable representing parameter x, which itself depends on coordinate (x_1, x_2) and integration variable ψ. However, as noted in light of (16) for $y = 0$, (x_1, x_2) can be replaced by quasipolar coordinates $(x, \psi - \theta)$. Thus traction σ itself can be found by dropping η, and (25a) is reduced to

$$\frac{\mathrm{K}}{\pi}(vp)\int_\Xi \sigma(\xi, \psi-\theta)\frac{d\xi}{\xi - x} + \Gamma\sigma(x, \psi-\theta) = \mu_0\frac{x}{r_0}. \tag{27}$$

Equation (27) is a Cauchy singular integral equation [Erdogan 1978]. Following a procedure used in [Brock 2012; 2013] and requiring that contact zone traction be bounded on C gives the solution

$$\sigma(x, \psi-\theta) = -\frac{\mu_0 \mathrm{M}_0 \mathrm{M}}{r_0\sqrt{\mathrm{A}_K^2 + \mathrm{A}_\Gamma^2}}(x_+ - x)^{1+\Omega}(x - x_-)^{-\Omega}, \tag{28a}$$

$$x_+ = -\Omega L, \quad x_- = -(1+\Omega)L. \tag{28b}$$

In (28) terms $(\Omega, \mathrm{A}_K, \mathrm{A}_\Gamma)$ are defined as

$$\Omega = -\frac{1}{2} + \frac{1}{\pi}\tan^{-1}\frac{\Gamma}{\mathrm{K}}, \tag{29a}$$

$$\mathrm{A}_K = \mathrm{M}_0\frac{A_1\mathrm{P}_+}{\sqrt{d_3 d_5}} + c_D^2 \mathrm{M} A(A+B), \tag{29b}$$

$$\mathrm{A}_\Gamma = \gamma(\mathrm{M}_0\mathrm{N} + \mathrm{M}\mathrm{N}_0)\cos(\psi-\theta). \tag{29c}$$

It is noted that $-\frac{1}{2} < \Omega < 0$ and $(\mathrm{M}, \mathrm{M}_0) \geq 0$ for subcritical V, so that (28a) also guarantees contact and does not involve tensile stress.

Contour of C. Equation (28b) defines, in part, contour $\Im$ and, because $\Omega = -\frac{1}{2}$ when $|\psi - \theta| = \pi/2$ and is an even function of $\psi - \theta$, C exhibits the symmetry of the sphere with respect to X. The unknown contact zone span L depends on c_0 (or c) and is also an even function of $\psi - \theta$. It is determined by requiring that (28a) be consistent with the resultant force system acting on the die. Therefore, here $(x_\pm, \sigma)$ are even functions of $\psi - \theta$, and also Y. Thus condition $F_Y = 0$ is automatically satisfied. The condition that there are resultant forces $F_X = \gamma F_3$ and F_3 is met when

$$\int_\Psi d\psi \int_\Xi \sigma(\xi, \psi)|\xi|\, d\xi = -F_3. \tag{30}$$

Here F_3 is specified and (30), therefore, is an integral equation for L. For given (c_0, θ), F_3 should be stationary with respect to (28a); that is,

$$\int_\Psi d\psi \int_\Xi \delta\sigma(\xi, \psi)|\xi|\, d\xi = 0. \tag{31}$$

This requirement is satisfied when at every $x_- < x < x_+$, $|\psi - \theta| < \pi/2$

$$\delta\sigma = \frac{\partial\sigma}{\partial x}\,\delta x + \frac{\partial\sigma}{\partial\psi}\,\delta\psi = 0. \tag{32}$$

Here ψ and x are held constant in the first and second coefficients, respectively, and $(\delta x, \delta\psi)$ are arbitrary. Differentiation of (28a) shows that

$$x = -(1 + 2\Omega)L: \quad \frac{\partial\sigma}{\partial x} = 0, \quad \frac{\partial^2\sigma}{\partial x^2} > 0. \tag{33a}$$

The second term then vanishes for $x = -(1 + 2\Omega)L$ if

$$-\frac{\partial}{\partial\psi}\left(\frac{\mathrm{M_0M}}{\sqrt{\mathrm{A_K^2} + \mathrm{A_\Gamma^2}}}QL\right) = 0, \qquad Q = (1 + \Omega)^{1+\Omega}(-\Omega)^{-\Omega}. \tag{33b}$$

Separation of variables and integration gives

$$L = \frac{Q_X}{Q}\,\frac{(\mathrm{M_0M})_X}{\mathrm{M_0M}}\,\frac{\sqrt{\mathrm{A_K^2} + \mathrm{A_\Gamma^2}}}{\sqrt{(\mathrm{A_K^2})_X + (\mathrm{A_\Gamma^2})_X}}L_X. \tag{34}$$

Subscript X signifies that a parameter is evaluated for $\psi = \theta$, that is, $c_X^0 = c_0$ (or $c_X = c$). For $L = L_Y$, that is, $|\psi - \theta| = \pi/2$, (34) gives

$$L_Y = \frac{Q_X(\mathrm{M_0M})_X}{\sqrt{(\mathrm{A_K^2})_X + (\mathrm{A_\Gamma^2})_X}}\left[c_D^2 + \frac{2\sqrt{d_1}\sqrt{2d_5 + \sqrt{d_1 d_3} + d_{13}}}{(\sqrt{d_1 d_3} + d_{13})\sqrt{d_5}\sqrt{\sqrt{d_1 d_3} - d_{13}}}\right]\frac{L_X}{c_D^2 - 1}. \tag{35}$$

Lengths (L_X, L_Y) are the span of contact zone C respectively along and perpendicular to the sliding path. The profile projected prior to sliding by a sphere on the plane $x_3 = 0$ is a circle. Equations (34) and (35) show that this shape is not preserved in the contact zone C. In addition, (28b) shows that only symmetry with respect to the sliding (positive X-)direction is preserved in the contact zone. Results (28) and (35), moreover, are sensitive to the dimensionless die sliding speed $(c_0 \neq 0)$. To illustrate this behavior values of the ratio L_Y/L_X are given in Table 1 for values of (γ, c_0). The sphere is ASTM-A913 Grade 450 steel with these properties [Beer et al. 2012]:

$$\mu_0 = 77.2\,\text{GPa}, \quad \rho_0 = 7860\,\text{kg/m}^3, \quad v_0 = 3134\,\text{m/s}.$$

The transversely isotropic half-space is a graphite epoxy with properties [Jones 1999]

$$\begin{aligned} &C_{11} = 13.9\,\text{GPa}, \quad C_{33} = 160.7\,\text{GPa}, \quad C_{13} = 6.44\,\text{GPa}, \quad C_{12} = 6.92\,\text{GPa}, \\ &C_{55} = 7.07\,\text{GPa}, \quad C_{66} = 3.5\,\text{GPa}, \quad \rho = 1688\,\text{kg/m}^3. \end{aligned}$$

In view of (5) and (6), the corresponding dimensionless parameters are

$$\begin{aligned} &d_1 = 0.1803, \quad d_3 = 2.0816, \quad d_{13} = 0.0834, \quad d_{12} = 0.0896, \\ &d_5 = 0.0916, \quad d_6 = 0.0453, \\ &c_D = 1.8554, \quad c = 0.4634 c_0. \end{aligned}$$

For $\psi = \theta$ the Rayleigh roots of $(\mathrm{M}, \mathrm{M}_0)$ are $c_0 = 0.9268$ and $c_0 = 0.6387$, respectively. Among terms (A, B, A_1, B_5, B_6), the branch point of B_6 is the minimum, which corresponds to $c_0 = 0.4595$. Thus, this value of c_0 is the maximum for subcritical sliding, that is, $V < 1440\,\text{m/s}$. Entries in Table 1 show contact zone geometry consistent with that for a rigid die sliding on an isotropic solid [Brock 2012] and on the surface of axial material symmetry for a transversely isotropic solid [Brock 2013]. That is, the contact zone is a noncircular oval, elongated in the direction of sliding. Such elongation is also found for an isotropic solid [Rahman 1996]. Table 1 entries show that, as in [Brock 2012; 2013], the elongation increases with sliding speed (c_0). Substitution of (28) and (34) in (30) gives, finally, an equation for L_X as a function of c_0:

$$F_3 = \frac{\mu_0}{r_0}\left(\frac{Q\mathrm{M}_0\mathrm{M}}{\sqrt{\mathrm{A}_\mathrm{K}^2 + \mathrm{A}_\Gamma^2}}\right)_X^3 L_X^3 \int_\Psi \frac{d\psi}{Q^2} \frac{\mathrm{A}_\mathrm{K}^2 + \mathrm{A}_\Gamma^2}{(\mathrm{M}_0\mathrm{M})^2} \int_\Omega^{1+\Omega} (1+\Omega-t)^{1+\Omega}(t-\Omega)^{-\Omega}|t|\,dt. \tag{36}$$

4. Transverse isotropy: Material symmetry axis in plane of surface

Traction distribution problem: Transform. In this case the material symmetry axis aligns with the positive x_2-direction, and elastic constants [Jones 1999] and related dimensionless parameters are given by

	$c_0 = 0.05$	$c_0 = 0.1$	$c_0 = 0.2$	$c_0 = 0.3$	$c_0 = 0.4$
$\gamma = 0.1$	0.5333	0.5282	0.5061	0.469	0.4102
$\gamma = 0.2$	0.5321	0.5271	0.5054	0.4678	0.4089
$\gamma = 0.5$	0.5197	0.5191	0.4974	0.4596	0.4007

Table 1. Ratio L_Y/L_X for values of γ and $c_0 < 0.4595$ $(c < \sqrt{d_6} = 0.2129)$.

(5) and

$$C_{33}=C_{11},\quad C_{66}=C_{44},\quad C_{23}=C_{12},\quad C_{22},\quad C_{11}-C_{13}-2C_{55}=0,\tag{37a}$$

$$d_1=\frac{C_{11}}{\mu_0},\quad d_2=\frac{C_{22}}{\mu_0},\quad d_4=\frac{C_{44}}{\mu_0},\quad d_5=\frac{C_{55}}{\mu_0},\quad d_{12}=\frac{C_{12}}{\mu_0},\quad d_{13}=\frac{C_{13}}{\mu_0},\tag{37b}$$

$$d_1-d_{13}-2d_5=0,\quad c=\sqrt{\frac{\rho}{\rho_0}}c_0,\quad c_0=\frac{v}{v_0}.\tag{37c}$$

Equations (A.5) and (37) give the homogeneous equation set

$$\begin{bmatrix} d_5\partial_3^2+\mathrm{X}_1 & (d_6+d_{12})\partial_1\partial_2 & (d_5+d_{13})\partial_1\partial_3 \\ (d_6+d_{12})\partial_1\partial_2 & d_6\partial_3^2+\mathrm{X}_2 & (d_6+d_{12})\partial_2\partial_3 \\ (d_5+d_{13})\partial_1\partial_3 & (d_6+d_{12})\partial_2\partial_3 & d_1\partial_3^2+\mathrm{X}_3 \end{bmatrix}\begin{bmatrix} u_1\\ u_2\\ u_3\end{bmatrix}=0,\tag{38a}$$

$$\mathrm{X}_1=d_1\partial_1^2+d_6\partial_2^2-c^2\partial_X^2,\quad \mathrm{X}_2=d_6\partial_1^2+d_2\partial_2^2-c^2\partial_X^2,\quad \mathrm{X}_3=d_5\partial_1^2+d_6\partial_2^2-c^2\partial_X^2.\tag{38b}$$

The same procedure based on (8) gives, for $x_3=0$, in place of (9), (12), and (13):

$$\hat{\boldsymbol{u}}=\boldsymbol{U}_+\exp(-\Omega_+x_3)+\boldsymbol{U}_-\exp(-\Omega_-x_3)+\boldsymbol{U}_5\exp(-\Omega_5x_3),\tag{39a}$$

$$(U_1^\pm,U_3^\pm)=(d_6+d_{12})p_2(-p_1,\Omega_\pm)U_\pm,\quad U_2^\pm=\big(A_6-\tfrac{1}{2}d_1P_\pm\big)U_\pm,\tag{39b}$$

$$U_1^5=\Omega_5U_5,\quad U_2^5=0,\quad U_3^5=p_1U_5,\tag{39c}$$

$$\frac{1}{\mu_0}\begin{bmatrix}\hat{\sigma}_{33}\\ \hat{\sigma}_{31}\\ \hat{\sigma}_{32}\end{bmatrix}=\begin{bmatrix} p_2C_3^+ & p_2C_3^- & -2d_5p_1\Omega_5\\ d_6D_{13}\Omega_+ & d_6D_{13}\Omega_- & T_5\\ D_{32}^+\Omega_+ & D_{32}^-\Omega_- & d_6p_1p_2\end{bmatrix}\begin{bmatrix}U_+\\ U_-\\ U_5\end{bmatrix}.\tag{39d}$$

The matrix coefficients in (39d) are given by

$$C_3^\pm=(d_6+d_{12})T_5-d_1(\Omega_\pm^2+p_1^2)-A_6,\tag{40a}$$

$$D_{13}=2d_5p_1p_2(d_6+d_{12}),\tag{40b}$$

$$D_{32}^\pm=(d_6+d_{12})p_2^2-d_1(\Omega_\pm^2+p_1^2)-A_6.\tag{40c}$$

For both (39) and (40) the following definitions hold:

$$\Omega_\pm=\sqrt{p_1^2+\frac{P_\pm}{2d_1d_6}}\sqrt{-1},\quad \Omega_5=\omega_5\sqrt{-1},\tag{41a}$$

$$P_\pm=d_1A_2+d_6A_6-(d_6+d_{12})^2p_2^2\pm\sqrt{[d_1A_2+d_6A_6-(d_6+d_{12})^2p_2^2]^2-4d_1d_6A_2A},\tag{41b}$$

$$A_6=p_2^2-c^2p_X^2,\quad A_2=d_2p_2^2-c^2p_X^2,\quad \omega_5=\sqrt{p_1^2+\frac{A_6}{d_5}}.\tag{41c}$$

As in the first problem, coefficients $(U_\pm,U_5)$ are obtained as functions of (p_1,p_2) by imposing the transform of condition (3) on the transforms given by (39). The transform $\hat{u}_3^0$ of the normal displacement for $x_3=0$ can then be written.

Transform inversion and sliding contact problem. Results (40) and (41) are relatively complicated in comparison with (10) and (11). For the purposes of illustration, therefore, the frictionless limit ($\gamma = 0$) is treated. Results analogous to those in Appendix A obtain, and the same transform inversion process used above is then used to reduce the sliding contact problem to a singular integral equation. The result is a normal contact zone traction that is bounded for $x_3 = 0$, $(x_1, x_2) \in C$:

$$\sigma(x, \psi, \psi - \theta) = \frac{\mu_0}{2\mathrm{K} r_0}\sqrt{L^2 - 4x^2}, \quad x_\pm = \pm\frac{L}{2}. \tag{42}$$

In (42), definition (19c) and (25b) are replaced with

$$\mathrm{K} = \left|\frac{\mathrm{A}_6}{\mathrm{M}}\right| \mathrm{B}_+\mathrm{B}_-(\mathrm{B}_+ + \mathrm{B}_-) + \frac{c_D^2 A}{\mathrm{M}_0}(A + B), \tag{43a}$$

$$\mathrm{M} = 4d_5^2 B_5 B_+ B_-(\mathrm{B}_+ + \mathrm{B}_-)\cos^2\psi - d_6 A_6(B_1^2 + \mathrm{B}_+\mathrm{B}_-)\sin^2\psi - Q_\mathrm{B}\mathrm{T}_5^2. \tag{43b}$$

Terms that arise in (42) and (43) are

$$\mathrm{T}_5 = \mathrm{A}_6 + 2d_5\cos^2\psi, \quad Q_\mathrm{B} = \frac{1}{d_1 d_6}(d_6 + d_{12})^2\sin^2\psi - \cos^2\psi - \frac{\mathrm{A}_2}{d_6} - \mathrm{B}_+\mathrm{B}_-, \tag{44a}$$

$$B_5 = \sqrt{\cos^2\psi + \frac{\mathrm{A}_6}{d_5}}, \quad B_1 = \sqrt{\cos^2\psi + \frac{\mathrm{A}_6}{d_1}}, \quad \mathrm{B}_\pm = \sqrt{\cos^2\psi + \frac{\mathrm{P}_\pm}{2d_1 d_6}}, \tag{44b}$$

$$\mathrm{P}_\pm = d_1\mathrm{A}_2 + d_6\mathrm{A}_6 - (d_6 + d_{12})^2\sin^2\psi \pm \sqrt{[d_1\mathrm{A}_2 + d_6\mathrm{A}_6 - (d_6 + d_{12})^2\sin^2\psi]^2 - 4d_1 d_6\mathrm{A}_2\mathrm{A}_6}, \tag{44c}$$

$$\mathrm{A}_6 = d_6\sin^2\psi - c_X^2, \quad \mathrm{A}_2 = d_2\sin^2\psi - c_X^2, \quad c_X = c\cos(\psi - \theta). \tag{44d}$$

Here $\mathrm{B}_+\mathrm{B}_-(\mathrm{B}_+ + \mathrm{B}_-) > 0$ for $(B_1, B_5, \mathrm{B}_\pm)$ real, and $(\mathrm{M}, \mathrm{A}_6)$ vanish for $|\psi, \theta| < \pi/2$ if

$$\tan\psi + \frac{c\cos\theta}{c\sin\theta \pm \sqrt{d_6}} = 0. \tag{45}$$

Thus, the first term in (43a) always gives a finite value. The second term in (43a) shows that A_6 cancels from u_3^0 in the isotropic limit. In any event (42) is finite and continuous, and guarantees a nontensile contact zone.

The anisotropy of the half-space surface is manifest in the definition (42)–(44). In particular, solution behavior now depends on orientation with respect to principal axes of both points in C and the path of the sliding sphere. Moreover, the definition of the critical sliding speed in terms of branch-point values and roots of $(\mathrm{M}, \mathrm{M}_0)$ is θ-dependent. The branch points of $(B_5, \mathrm{B}_\pm)$ are relevant and are given, respectively, in terms of dimensionless speed c_0 as

$$(c_0)_{56} = \sqrt{\frac{\rho_0}{\rho}}\sqrt{d_6\sin^2\theta + d_5\cos^2\theta}, \tag{46a}$$

$$(c_0)_\pm = \frac{1}{2}\sqrt{\frac{\rho_0}{\rho}}\left[\sqrt{d_6 + \mathrm{P} + \mathrm{P}_6} \pm \sqrt{d_6 + \mathrm{P} - \mathrm{P}_6}\,\right], \tag{46b}$$

$$\mathrm{P} = d_1\cos^2\theta + d_2\sin^2\theta, \tag{46c}$$

$$\mathrm{P}_6 = \sqrt{4\mathrm{P}^2 + [d_6^2 - 2d_1 d_2 - (d_6 + d_{12})^2]\sin^2 2\theta}. \tag{46d}$$

$\theta =$	$0°$	$30°$	$45°$	$60°$	$90°$
$(c_{56})_0$	0.4595	0.5147	0.5646	0.6104	0.653
$(c_+)_0$	0.9163	1.6743	2.2576	2.7193	3.113
$(c_-)_0$	0.653	0.8222	0.7719	0.7153	0.653

Table 2. Values of c_0 associated with solution branch points for various θ. Note that $A(1.8554) = 0$, $B(1) = 0$, and $\mathrm{M}_0(0.9268) = 0$.

Contour C. Expressions analogous to (34) and (36) can be obtained for this case:

$$L = \frac{\mathrm{K}}{\mathrm{K}_X} L_X, \qquad F_3 = \frac{L_X^3}{12\mathrm{K}_X^3} \frac{\mu_0}{r_0} \int_\Xi d\psi\, \mathrm{K}^2. \tag{47}$$

In (47) subscript X signifies a quantity evaluated for $\psi = \theta$. In this case, however, terms in (43) and (44) are not, in general, even functions with respect to the X-direction; for example, for $\mathrm{M}(\psi, \psi - \theta)$ we have $\mathrm{M}(\theta + \phi, \phi) \neq \mathrm{M}(\theta - \phi, \phi)$ for $\phi \neq \pi/2$. Thus contact zone C symmetry may not involve the (X, Y)-axes. In this case, therefore, it is perhaps more illustrative to study the ratio

$$L_\Phi / L_X = \mathrm{K}_\Phi / \mathrm{K}_X. \tag{48}$$

As in (34) and (47) L_X is the contact zone span along the direction θ of sliding. Length L_Φ is the span along lines that make an angle ϕ with respect to the X-direction, that is, $\psi = \theta + \phi$ where $|\phi| \leq \pi/2$. The sphere has the same properties as used for the first problem, but orientation of the graphite epoxy [Jones 1999] now gives dimensionless parameters

$$d_1 = 0.1831, \quad d_2 = 2.0816, \quad d_{13} = 0.0896, \quad d_{12} = 0.0834, \quad d_5 = 0.0453, \quad d_6 = 0.0916.$$

Based on these, Table 2 presents dimensionless parameters $(c_0)_{56}$ and $(c_0)_\pm$ associated with various values of θ. It is noted that $(c_0)_{56} \leq (c_0)_\pm$. It can also be shown that ratio $|\mathrm{M}/\mathrm{A}_6| \neq 0$ for $0 < c_0 < (c_0)_{56}$ and that the second (isotropic) term in (43a) does not become singular until $c_0 = 0.9268$. Therefore $v = (c_0)_{56} v_0$ defines the critical sliding speed. Table 3 presents values of ratio (48) for $\theta = 45°$ and various values of ϕ. Table 2 shows that critical sliding speed for this direction is 1769 m/s. In the first problem the value was 1440 m/s for all sliding directions.

Entries in Table 1 depicted the contact zone as a noncircular oval, elongated in the direction of sliding. In this problem $\phi = 0°$ and $\phi = \pm 90°$ define the direction of sliding and its normal, and $\phi = \pm 45°$ define the (x_2, x_1)-principal material axes. Entries in Table 3 show that the contact zone for $c_0 = 0.05$ has an oval shape, but elongation is defined in terms of the principal axes, not the sliding direction ($\theta = 45°$). As c_0 is increased, however, the contact zone "rotates" and forms an oval elongated in the sliding direction, as in the first problem. This behavior is consistent with that for the rigid sliding sphere [Brock 2013]; that is, for low sliding speed the contact zone contour is largely determined by the orientation of the in-plane principal axes. For higher speeds, the direction of sliding becomes important.

5. Summary and comments

Combining quasipolar coordinates with an analysis defined in terms of Cartesian coordinates does result in solutions of a hybrid nature. However, analytical expressions for contact zone traction in the quasipolar

$\phi°$	$c_0 = 0.05$	$c_0 = 0.1$	$c_0 = 0.2$	$c_0 = 0.3$	$c_0 = 0.4$
90	1.0218	1.0002	0.9113	0.7917	0.5945
67.5	0.8743	0.856	0.7859	0.6913	0.5279
45	0.823	0.8098	0.7536	0.6797	0.5403
22.5	0.8778	0.8668	0.8233	0.7748	0.6657
0	1.0	1.0	1.0	1.0	1.0
−22.5	1.2124	1.21	1.2103	1.257	1.4348
−45	1.2274	1.2168	1.1705	1.1286	1.023
−67.5	1.2058	1.1842	1.0937	0.973	0.7557
−90	1.2168	1.191	1.0852	0.9428	0.7079

Table 3. Ratio L_Φ/L_X for $\gamma = 0$, $\theta = 45°$, ϕ and $c_0 < (c_0)_{56} = 0.5646$. Note that $\psi = \theta + \phi$.

system are readily extracted. In any event, the approach is adopted here in order to address problems that may not exhibit axial symmetry. The factor cancellation procedure adopted here follows that of the 2D analysis of sliding on a transversely half-plane surface [Brock 2002]. A more compact solution expression is the result, but care must then be used in comparing it with that for the isotropic limit case, for example, as in [Rahman 1996].

The assumption that key geometric features of the projection of die profile onto the contact surface are preserved in the contact zone shape, or that the zone is essentially elliptical, is often accurate [Johnson 1985; Hills et al. 1993]. Here, however, in addition to requiring a bounded traction on the zone boundary, the resultant compressive force is required to be stationary with respect to the traction. The expressions for contact zone geometry that result from these requirements, and calculations based on them, indicate that the contact zone is often a distortion of the projection. This result is consistent with those in [Brock 2012; 2013].

For the case of the material symmetry axis for a transversely isotropic material coinciding with the half-space surface normal, the contact zone shape represents in a sense an elongation of a sphere profile along the line of sliding; see [Rahman 1996; Brock 2012; 2013]. The effect is sensitive to sliding speed, and the presence of friction prevents replication by the contact zone of projection symmetry, other than that with respect to this line.

For the case of the material symmetry axis lying in the surface plane, solution response in the contact zone depends on both sliding direction orientation and location in the contact zone with respect to the principal material axes. Contact zone elongation is along a principal material axis for low sliding speeds. As sliding speed is increased, however, elongation is more consistent with isotropic behavior, that is, elongation is in the sliding direction. This behavior is also consistent with [Brock 2013] but the changes in shape during the transition from one behavior to the other are more pronounced here. This contrast suggests that analysis based on the rigid die is indeed a first step.

For frictionless sliding by a sphere, calculations for L_Y/L_X in Table 1 could be used to provide semiminor and semimajor axis measures for the elliptical contact zone model, for example, as in [Johnson 1985]. As noted above, friction may preserve profile symmetry only with respect to translation direction. However, the data in Table 1 indicates that the elliptical contact zone model may still be a useful approximation. In the second problem treated here, contact zone symmetry may not coincide with that exhibited by the circular profile for the sphere. Calculations in Table 3 might still prove useful for the contact zone shape that is assumed; similar conclusions are reached in [Brock 2012; 2013].

This study also shows that, in a 3D analysis of transverse isotropy, Rayleigh speeds may not be critical. Specifically, the Rayleigh speeds for both a sphere and a half-space whose surface normal is the axis of material symmetry can be obtained. However, for the graphite epoxy material [Jones 1999] chosen for calculation, the value corresponds to a transonic speed, and the speed for steel exceeds that value. For the surface that contains the material symmetry axis, the Rayleigh function for such a material does not vanish in the subsonic sliding speed range. Again, moreover, the Rayleigh speed for steel corresponds to a transonic speed in the half-space.

In closing, it is recognized that sliding contact between an isotropic sphere and a transversely isotropic half-space with a surface that coincides with a principal material plane is a special case. A more tractable mathematical problem arises and, as a result, so does a solution in a simple analytical form. Nevertheless, anisotropic bodies are often composites, and shaped so that their surfaces do coincide with a principal plane [Jones 1999]. Moreover, the second problem may give insight into the response of materials with greater degrees of anisotropy.

Appendix A

For the homogeneous and linear elastic anisotropic solid, the stress and strain measure (σ_k, ϵ_k) in contracted notation is related by [Jones 1999]:

$$\sigma_k = C_{kl}\epsilon_l, \quad C_{kl} = C_{lk}. \tag{A.1}$$

Indices (k, l) take on values $(1, 2, 3, 4, 5, 6)$ and the 21 elastic parameters are constants. These measures correspond to those in the Cartesian basis, for $k = (1, 2, 3)$, as

$$\sigma_k = \sigma_{kk}, \quad \epsilon_k = \partial_k u_k. \tag{A.2}$$

For $k = (4, 5, 6)$, the correspondence is

$$\sigma_4 = \sigma_{23} = \sigma_{32}, \quad \epsilon_4 = \partial_2 u_3 + \partial_3 u_2, \tag{A.3a}$$

$$\sigma_5 = \sigma_{31} = \sigma_{13}, \quad \epsilon_5 = \partial_3 u_1 + \partial_1 u_3, \tag{A.3b}$$

$$\sigma_6 = \sigma_{12} = \sigma_{21}, \quad \epsilon_6 = \partial_1 u_2 + \partial_2 u_1. \tag{A.3c}$$

Here (u_k, ∂_k) are k-components of the displacement and gradient vector $(\boldsymbol{u}, \nabla)$. The strain energy density is positive for (A.1) when $\epsilon_k^T C_{kl}\epsilon_l > 0$. This condition, in turn, is satisfied when [Hohn 1965; Ting 1996]

$$\begin{vmatrix} C_{11} & C_{21} & \cdots & C_{1n} \\ C_{21} & C_{22} & \cdots & C_{2n} \\ \vdots & \vdots & \ddots & \vdots \\ C_{n1} & C_{2n} & \cdots & C_{nn} \end{vmatrix} > 0 \quad (n \le 6). \tag{A.4}$$

In view of (1), (2), and (A.1)–(A.3), the linear momentum balance in the translating Cartesian basis takes the form

$$\nabla_{kl}\epsilon_l - \rho v^2 \partial_X^2 u_k = 0, \tag{A.5a}$$

$$\begin{bmatrix} \nabla_{1l} \\ \nabla_{2l} \\ \nabla_{3l} \end{bmatrix} = \begin{bmatrix} C_{l1} & C_{l6} & C_{l5} \\ C_{l6} & C_{l2} & C_{l4} \\ C_{l5} & C_{l4} & C_{l3} \end{bmatrix} \begin{bmatrix} \partial_1 \\ \partial_2 \\ \partial_3 \end{bmatrix}. \tag{A.5b}$$

Here ρ is the mass density, $k = (1, 2, 3)$, $l = (1, 2, 3, 4, 5, 6)$, and the summation convention applies.

Appendix B

For $x_3 = 0$, (9) and (12) give the formal result

$$\hat{u}_3^0 = (d_5\Omega_+^2 + \omega_1^2)U_+ + (d_5\Omega_-^2 + \omega_1^2)U_-. \tag{B.1}$$

In view of (13) the solutions for $(U_\pm, U_6)$ and, therefore, the coefficients in (B.1) are functions of polynomials in $(\Omega_\pm, \Omega_6)$. These can be factored so that

$$\hat{u}_3^0 = d_5^2(d_5 + d_{13})(\Omega_+ - \Omega_-)\Omega_6\omega_1 \frac{P}{\Delta}\left[N\left(p_1\frac{\hat{\tau}_1}{\mu_0} + p_2\frac{\hat{\tau}_2}{\mu_0}\right) - \omega_1(\Omega_+ + \Omega_-)\frac{\hat{\sigma}}{\mu_0}\right], \tag{B.2a}$$

$$N = \omega_1 - \frac{d_{13}\omega_5}{\sqrt{d_3 d_5}}. \tag{B.2b}$$

Term Δ is the determinant of the matrix in (13a) and can also be factored:

$$\Delta = d_5^2(d_5 + d_{13})\omega_1\Omega_6 P(\Omega_+ - \Omega_-)M, \tag{B.3a}$$

$$M = \omega_1\omega_5\left(\omega_5 + \sqrt{\frac{d_3}{d_5}}\omega_1\right) - \left(d_5\omega_1 + \frac{d_{13}^2\omega_5}{\sqrt{d_3 d_5}}\right)P. \tag{B.3b}$$

Use of (B.3a) in (B.2a) leads, upon factor cancellation, to a more compact form. Similar results hold for the isotropic solid with mass density ρ_0, the shear modulus μ_0, and the rotational wave speed v_0, that is,

$$d_2 = d_1 = c_D^2, \quad d_5 = d_6 = 1, \quad d_{12} = d_{13} = c_D^2 - 2. \tag{B.4}$$

It can be shown that (11) and (12) reduce to

$$\Omega_+ = \omega_D\sqrt{-1}, \qquad \Omega_- = \Omega_6 = \omega\sqrt{-1}, \qquad T = 2P - c_0^2 p_X^2, \tag{B.5a}$$

$$\omega_D = \sqrt{P - \frac{c_0^2}{c_D^2}p_X^2}, \qquad \omega_5 = \omega = \sqrt{P - c_0^2 p_X^2}, \tag{B.5b}$$

$$C_3^+ = -(c_D^2 - 1)T\omega_D\sqrt{-1}, \quad D_3^+ = 2(c_D^2 - 1)\omega^2, \tag{B.5c}$$

$$C_3^- = -2(c_D^2 - 1)\omega P\sqrt{-1}, \quad D_3^- = (c_D^2 - 1)T. \tag{B.5d}$$

Parameter c_D is the dimensionless dilatational wave speed, and the determinant corresponding to Δ is

$$\omega_D\omega P(c_D^2 - 1)^2(4P\omega_D\omega - T^2). \tag{B.6}$$

The last term is the isotropic Rayleigh function [Brock 2012]. This term and the isotropic limit of (B.3b) can be written as, respectively,

$$\frac{\omega_D-\omega}{c_D^2-1}\times\omega[c_D^4\omega_D^2-(c_D^2-1)^2P]-\omega_D c_D^2 c_0^2 p_X^2, \tag{B.7a}$$

$$\frac{\omega}{c_D}[c_D^4\omega_D^2-(c_D^2-1)^2P]-\omega_D c_D c_0^2 p_X^2. \tag{B.7b}$$

Equation (B.7a) demonstrates that the nonzero roots of the isotropic Rayleigh function are also roots of the second factor. This implies that Δ is the transversely isotropic Rayleigh function, and that its nonzero roots will also be roots of factor M, where dimensionless sliding speeds (c, c_0) are related by (6b).

Appendix C

Consider integrals involving real parameters (X, Y) over the entire $\mathrm{Im}(p)$-axis P:

$$\frac{1}{2\pi i}\int_{\mathrm{P}}|p|\left(1,\frac{\sqrt{-p}}{\sqrt{p}}\right)\exp[pX-Y\sqrt{-p}\sqrt{p}\,]\frac{dp}{p}\quad (Y\geq 0). \tag{C.1}$$

$\mathrm{Re}(\sqrt{\pm p})\geq 0$ in the p-plane with, respectively, branch cuts $\mathrm{Im}(p)=0, \mathrm{Re}(p)<0$ and $\mathrm{Im}(p)=0$, $\mathrm{Re}(p)>0$. Specifically, for $\mathrm{Re}(p)=0+$ and, respectively, $\mathrm{Im}(p)=q>0$ and $\mathrm{Im}(p)=q<0$:

$$\sqrt{-p}=\left|\frac{q}{2}\right|^{1/2}(1\mp i),\qquad \sqrt{p}=\left|\frac{q}{2}\right|^{1/2}(1\pm i). \tag{C.2}$$

Use of (C.2) reduces (C.1) to

$$\frac{1}{i\pi}\int_0^\infty(\cos qX,\sin qX)\exp(-Yq)\,dq. \tag{C.3}$$

From the standard [Peirce and Foster 1956] tables (C.3) is evaluated as

$$\frac{1}{i\pi}\left(\frac{Y}{X^2+Y^2},\frac{X}{X^2+Y^2}\right). \tag{C.4}$$

It is noted in [Stakgold 1967] that

$$\frac{1}{\pi}\frac{Y}{X^2+Y^2}\to\delta(X)\quad (Y\to 0). \tag{C.5}$$

Here δ is the Dirac function.

References

[Ahmadi et al. 1983] N. Ahmadi, L. M. Keer, and T. Mura, "Non-Hertzian contact stress analysis for an elastic half-space: normal and sliding contact", *Int. J. Solids Struct.* **19**:4 (1983), 357–373.

[Beer et al. 2012] F. P. Beer, E. R. Johnston, Jr., J. T. DeWolf, and D. F. Mazurek, *Mechanics of materials*, 6th ed., McGraw-Hill, New York, 2012.

[Brock 2002] L. M. Brock, "Exact analysis of dynamic sliding indentation at any constant speed on an orthotropic or transversely isotropic half-space", *J. Appl. Mech. (ASME)* **69**:3 (2002), 340–345.

[Brock 2012] L. M. Brock, "Two cases of rapid contact on an elastic half-space: sliding ellipsoidal die, rolling sphere", *J. Mech. Mater. Struct.* **7**:5 (2012), 469–483.

[Brock 2013] L. M. Brock, "Rapid sliding contact in 3D by an ellipsoidal die on transversely isotropic half-spaces with surfaces on different principal planes", *J. Appl. Mech.* (*ASME*) **81**:3 (2013), Article ID #031005.

[Erdogan 1978] F. Erdogan, "Mixed boundary value problems in mechanics", pp. 1–86 in *Mechanics today*, vol. 4, edited by S. Nemat-Nasser, Pergamon, New York, 1978.

[Hartnett 1980] M. J. Hartnett, "A general numerical programming method for design of elastic bodies in contact", pp. 51–66 in *Solid contact and lubrication* (Chicago, 1980), edited by H. S. Cheng and L. M. Keer, Applied Mechanics Division **39**, American Society of Mechanical Engineers, New York, 1980.

[Hertz 1882] H. Hertz, "Ueber die Berührung fester elastischer Körper", *J. Reine Angew. Math.* **1882**:92 (1882), 156–171. Translated as "On the contact of elastic solids", pp. 146–162 in *Miscellaneous papers*, edited by P. Lenard, Macmillan, London, 1896.

[Hills et al. 1993] D. A. Hills, D. Nowell, and A. Sackfield, *Mechanics of elastic contacts*, Butterworth-Heinemann, Oxford, 1993.

[Hohn 1965] F. E. Hohn, *Elementary matrix algebra*, Macmillan, New York, 1965.

[Johnson 1985] K. L. Johnson, *Contact mechanics*, Cambridge University Press, 1985.

[Jones 1999] R. M. Jones, *Mechanics of composite materials*, 2nd ed., Taylor & Francis, Philadelphia, 1999.

[Kalker 1990] J. J. Kalker, *Three-dimensional elastic bodies in rolling contact*, Kluwer, Dordrecht, 1990.

[Peirce and Foster 1956] B. O. Peirce and R. M. Foster, *A short table of integrals*, 4th ed., Ginn, New York, 1956.

[Rahman 1996] M. Rahman, "Hertz problem for a rigid punch moving across the surface of a semi-infinite elastic solid", *Z. Angew. Math. Mech.* **47**:4 (1996), 601–615.

[Sneddon 1972] I. N. Sneddon, *The use of integral transforms*, McGraw-Hill, New York, 1972.

[Stakgold 1967] I. S. Stakgold, *Boundary value problems of mathematical physics*, vol. 1, Macmillan, New York, 1967. Reprinted in *Classics in Applied Mathematics* **29**, SIAM, Philadelphia, 2000.

[Ting 1996] T. C. T. Ting, *Anisotropic elasticity: theory and applications*, Oxford Engineering Science Series **45**, Oxford University Press, New York, 1996.

Received 10 Jun 2013. Accepted 23 Sep 2013.

LOUIS MILTON BROCK: louis.brock@uky.edu
Mechanical Engineering, University of Kentucky, 265 RGAN, Lexington, KY 40506-0503, United States

JOURNAL OF MECHANICS OF MATERIALS AND STRUCTURES

msp.org/jomms

Founded by Charles R. Steele and Marie-Louise Steele

See msp.org/jomms for submission guidelines.

JoMMS (ISSN 1559-3959) at Mathematical Sciences Publishers, 798 Evans Hall #6840, c/o University of California, Berkeley, CA 94720-3840, is published in 10 issues a year. The subscription price for 2013 is US $555/year for the electronic version, and $705/year (+$60, if shipping outside the US) for print and electronic. Subscriptions, requests for back issues, and changes of address should be sent to MSP.

JoMMS peer-review and production is managed by EditFlow® from Mathematical Sciences Publishers.

PUBLISHED BY

mathematical sciences publishers

nonprofit scientific publishing

http://msp.org/

Journal of Mechanics of Materials and Structures

Volume 8, No. 8-10 October-December 2013